ChemPubSoc Europe

DOI: 10.1002/cbic.201500560

CHEMBIOCHEM Communications

Cell-Like Nanostructured Environments Alter Diffusion and Reaction Kinetics in Cell-Free Gene Expression

Maike M. K. Hansen,[a] Sabine Paffenholz,[a, b] David Foschepoth,[a] Hans A. Heus,[a] Julian Thiele,*[a, c] and Wilhelm T. S. Huck*[a]

In highly crowded and viscous intracellular environments, the kinetics of complex enzymatic reactions are determined by both reaction and diffusion rates. However in vitro studies on transcription and translation often fail to take into account the density of the prokaryotic cytoplasm. Here we mimic the cellular environment by using a porous hydrogel matrix, to study the effects of macromolecular crowding on gene expression. We found that within microgels gene expression is localized, transcription is enhanced up to fivefold, and translation is enhanced up to fourfold. Our results highlight the need to consider the role of the physical environment on complex biochemical reactions, in this case macromolecular crowding, nanoscale spatial organization, and confinement.

The intracellular environment of a cell differs greatly from the conditions typically used to study complex biochemical reactions ex vivo. Living cells contain macromolecules at up to 200–300 mg mL^{-1}, and diffusion rates as well as non-covalent interactions between macromolecules are strongly influenced by macromolecular crowding.[1–3] Moreover, the cellular cytoplasm has been shown to behave as a glass-forming liquid with increasing particle size.[4] This strongly affects the diffusion dynamics of cellular components, such as bacterial mRNA, which rarely disperses from the site of production.[5] Therefore, both DNA and mRNA targets can be seen as immobile in bacterial cells, rather than freely diffusing in solution, as in typical in vitro experiments.[6] Although our understanding of the physical nature of the intracellular environment continuously improves, it remains unclear how confinement, crowding, and localization impact on transcription and translation kinetics.[6–9]

[a] M. M. K. Hansen, S. Paffenholz, D. Foschepoth, Dr. H. A. Heus, Dr. J. Thiele, Prof. Dr. W. T. S. Huck
Radboud University, Institute for Molecules and Materials
Heyendaalseweg 135, 6525 AJ Nijmegen (The Netherlands)
E-mail: w.huck@science.ru.nl

[b] S. Paffenholz
Present address: Rhine–Waal University of Applied Sciences
Marie-Curie-Strasse 1, 47533 Kleve (Germany)

[c] Dr. J. Thiele
Present address: Department of Nanostructured Materials and Leibniz Research Cluster (LRC)
Leibniz-Institut für Polymerforschung Dresden e. V.
Hohe Strasse 6, 01069 Dresden (Germany)
E-mail: thiele@ipfdd.de

Supporting information for this article is available on the WWW under http://dx.doi.org/10.1002/cbic.201500560.

The kinetics of chemical and enzymatic reactions depend on the interaction probability of reactants.[10,11] This probability depends on reactant diffusivity, which is strongly influenced by the environment in which the reaction takes place.[6,12,13] Especially in confined systems where small numbers of reactants are involved and the movement of molecules is very slow (e.g., in cells), the environment is considered to have a large impact on kinetics.[10,14] It has been shown both in vivo[15] and in silico[10] that cellular gene expression, unlike gene expression in dilute solution,[16] experiences "geometry-controlled" kinetics: the combination of the maze-like nature of the cellular environment and an immobile DNA target.[10,17] Over short distances and small timescale, the mean squared displacement of molecules becomes sublinear; this anomalous diffusion is also termed "subdiffusion".[18] An important consequence of this form of diffusion (often underestimated when performing experiments on the nanoscale is that molecules remain longer at their initial positions and are more likely to rebind to an earlier target, if the target is stationary.[10,17,19] By following in vitro transcription (IVT) and in vitro transcription/translation (IVTT) separately, we studied the effects that macromolecular crowding has on gene expression in a porous hydrogel matrix with an immobile target, and compared these effects to those for typical bulk reactions with a mobile target.

To mimic geometry-controlled transcription and translation in a synthetic system, we covalently coupled DNA to monodisperse hydrogel beads (25 μm diameter; Figure 1 A) by thiol-Michael addition, as we have previously described.[20] Hydrogel is composed of hyaluronic acid (HA) cross-linked with polyethylene glycol diacrylate (PEGDA) to form polymer networks with large pore sizes, thus allowing even the largest components of the expression system (prokaryotic ribosomes: diameter ~34 nm) to enter the hydrogel.[21] The DNA-functionalized particles were then loaded into larger droplets (diameter 50 μm) that contained an *Escherichia coli*-based cell-free expression system (Figure 1 B).[13,22,23] By immobilizing DNA within a porous hydrogel matrix (Figure 1 C), we were able to systematically study the kinetics of both IVT and IVTT under geometry-controlled conditions. First, we determined the effect of the immobilization of DNA in the hydrogels. We used fluorescent recovery after photobleaching (FRAP) to assess diffusive dynamics in two systems: DNA coupled to hydrogel particles encapsulated in 30 pL droplets, and freely diffusing DNA ("bulk solution"). T7 RNA polymerase (T7 RNAP) transcribed DNA into mRNA containing a 32-repeat unit of a target sequence recognized by a molecular beacon (see Experimental Section), thus allowing us to visualize mRNA.[24] Diffusion of

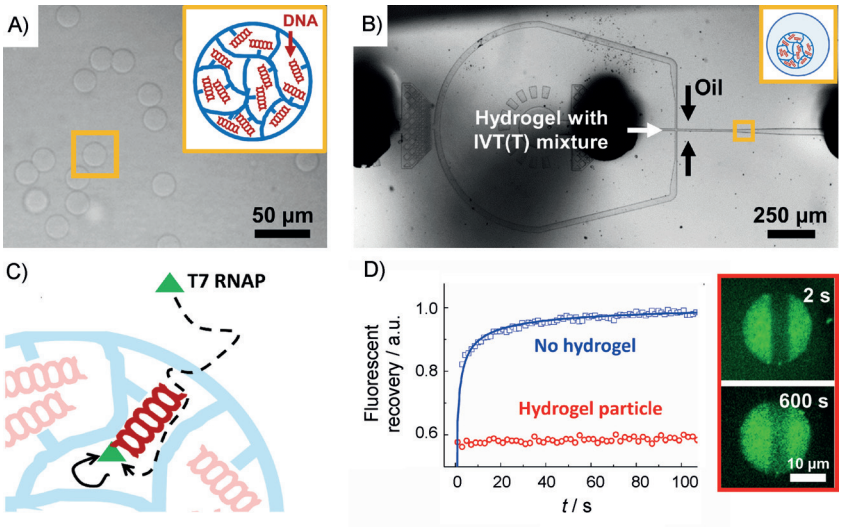

Figure 1. Fabrication of a microgel-loaded water-in-oil emulsion prepared by droplet microfluidics. A) Bright-field microscopy image of monodisperse hyaluronic acid microgels in water. Covalently attached DNA is homogeneously distributed throughout the hydrogel network. B) Encapsulation of DNA-functionalized microgel particles into microdroplets containing all necessary components for performing IVT or IVTT. C) The maze-like hydrogel allows geometry-controlled kinetics. T7 RNA polymerase (RNAP) finds its immobile DNA target. D) FRAP analysis of mRNA distribution during IVT in DNA-functionalized hydrogel particles and bulk solution (left), and example DNA-functionalized hydrogel particles during FRAP (right).

mRNA in bulk solution (Figure 1D blue squares) showed a clear recovery curve. However, there was no fluorescence recovery in the hydrogel beads (Figure 1D red circles), thus clearly indicating that the hydrogel environment prevents diffusion of mRNA.

To shed light on the effect of macromolecular crowding on gene expression in the two environments, Ficoll 70 was added as a non-interacting macromolecular crowding agent.[2,25] IVT reaction kinetics were determined at different Ficoll concentrations in 30 pL droplets containing one DNA-functionalized hydrogel particle, and in 30 μL bulk reactions with freely diffusing DNA (bulk solution).

We observed a strong increase in mRNA production with increasing Ficoll concentration in droplets containing the gel beads (Figure 2A). The rates of mRNA production were calculated from a fit to the linear part of the expression curve for both the hydrogel particles and the unconfined bulk IVT system. mRNA production rates in the gel beads increased fivefold upon addition of 150 mg mL^{-1} Ficoll (Figure 2B). In contrast, transcription rates from freely diffusing DNA in solution decreased with increasing Ficoll concentrations (Figure 2C). To understand the effects of a crowded environment on transcription, we carried out a detailed kinetic analysis. We assumed Michaelis–Menten kinetics with the following rate equation for transcription [Equation (1)]:

$$V_{Tx} = \frac{V_{max,Tx}[DNA]}{K_{M,Tx} + [DNA]} \quad (1)$$

where V_{Tx} is the transcription rate, $V_{max,Tx}$ is the maximum rate achieved by the system ([enzyme]$\times k_{cat}$, where [enzyme] is the initial enzyme concentration), $K_{M,Tx}$ is the Michaelis constant for transcription. The DNA concentration was 5 nM for both the microgel and bulk solution experiments. The $K_{M,Tx}$ and $V_{max,Tx}$ values for the dilute bulk environment (i.e., DNA freely diffusing in solution) were evaluated at 24 nM and 1.2 nM min^{-1} respectively (Figure S6 in the Supporting Information). The values for transcription rates inside microgel beads were similar, therefore in the absence of macromolecular crowding, hydrogel has no significant effect on the kinetics. When Ficoll is added, we can no longer assume standard Michaelis–Menten kinetics, and diffusion kinetics of reactants have to be taken into account when defining $K_{M,Tx}^{eff}$ [Eq. (2)]:[26]

$$K_{M,Tx}^{eff} = \frac{k_{cat} + k_{off}}{k_{on}} + \frac{k_{cat}}{k_{diff}} \quad (2)$$

where the term on the right takes into account the dependency of $K_{M,Tx}^{eff}$ on diffusion, and the term on the left is the standard definition of the Michaelis constant (for calculations see the Supporting Information). The addition of crowding agent slows diffusion,[27] thus lowering k_{diff}. We calculated values for k_{diff} based on the viscosity (η) of Ficoll, and the model predicts increased $K_{M,Tx}^{eff}$ values for increasing Ficoll concentration (Figure S6). These adjusted $K_{M,Tx}^{eff}$ values provide a good fit for the observed transcription rates in a freely diffusing DNA solution with increasing Ficoll concentration (Figure 2C blue line). However we could not fit transcription rates for gel beads from the same $K_{M,Tx}^{eff}$ values (Figure 2B red squares). We therefore fitted the increase in transcription rates with Equation (1), by defining $K_{M,Tx}^{eff}$ as [Eq. (3)]:

$$K_{M,Tx}^{eff} = K_{M,Tx} \exp(-a \times [Ficoll]) \quad (3)$$

We obtained a value of 0.017 ($\pm$0.002) for a. The decrease in $K_{M,Tx}^{eff}$ (and thus faster reaction rate) with increasing Ficoll

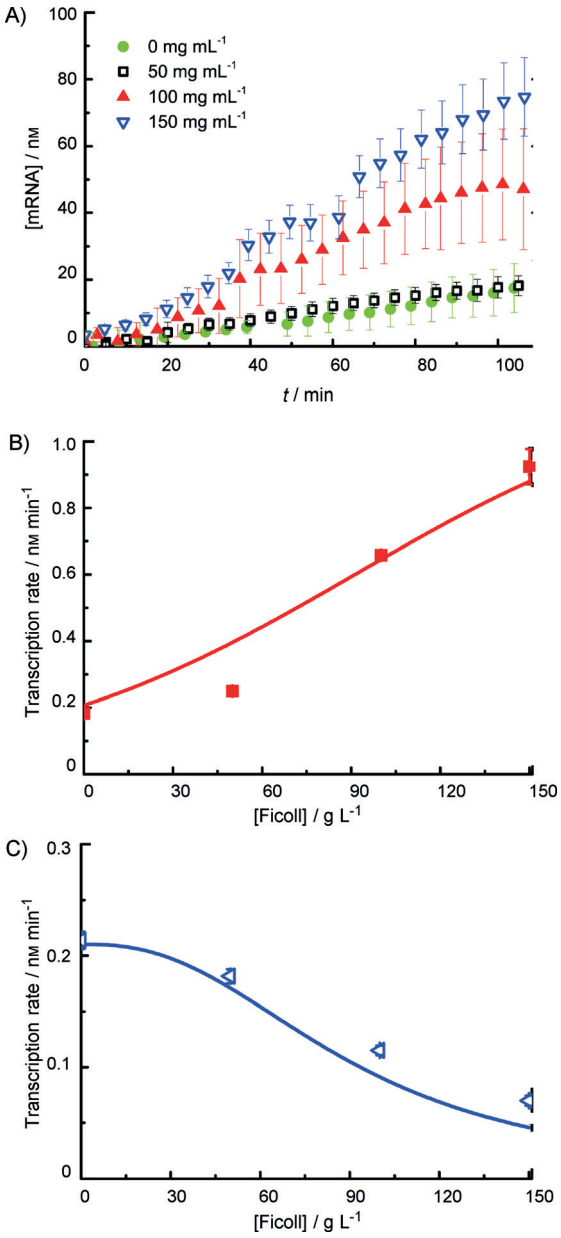

Figure 2. The dependence of in vitro transcription kinetics on macromolecular crowding in a cell-like environment or in bulk solution. A) Concentration of mRNA over time inside DNA-functionalized microgels containing 0 to 150 mg mL^{-1} Ficoll (mean ± SD, n = minimum of 2 droplets containing beads). Transcription rates for B) confined DNA-functionalized microgels and C) bulk solution, with error bars representing the standard error (SE). Solid lines represent extended Michaelis–Menten models for gene transcription with DNA as single substrate under the influence of macromolecular crowding.

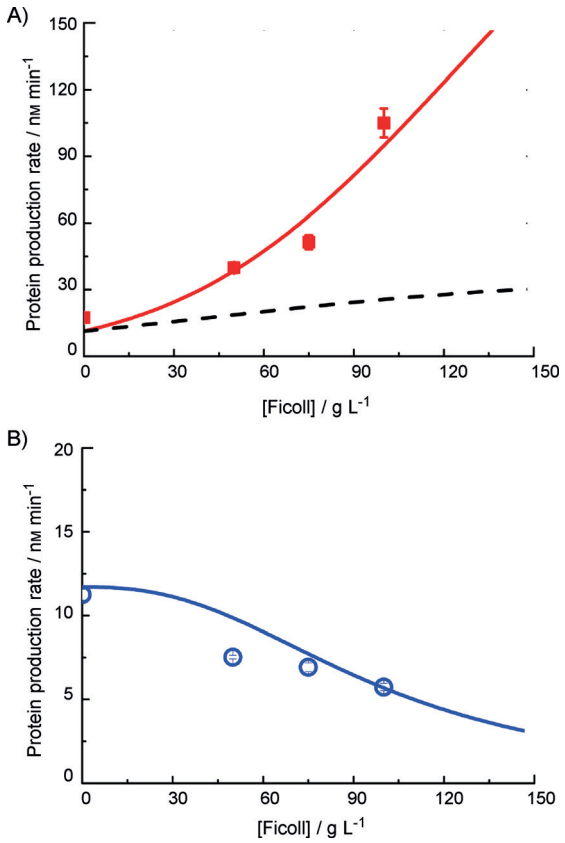

Figure 3. A) Coupled transcription and translation in microgels fitted to a Michaelis–Menten model for transcription-translation taking into account solely the increased transcription rates from Figure 2 (-----) or taking into account an additional decrease in $K_{M,TI}$ (——). B) Coupled transcription and translation rates in bulk solution (○) can be explained by the decreased in transcription rates from Figure 2. Error bars represent standard error (SE).

concentration is associated with the architecture of the microgel beads: the maze-like crowded environment leads to higher probabilities of reactants meeting[10] and macromolecular crowding favors the bound state of T7 RNAP.[25]

Additionally we studied IVTT with enhanced green fluorescent protein (eGFP) in hydrogel particles. We determined protein production rates in the presence of Ficoll from the respective expression curves (Figure S8). The rate increased from 0.02 μM min^{-1} without Ficoll to 0.11 μM min^{-1} at 100 mg mL^{-1} Ficoll (Figure 3 A, red squares). To rationalize these results, we modeled transcription and translation as a two-step Michaelis–Menten reaction.[13,28] In the transcription step [Eq. (1)] we used $V_{max,Tx} = 1.4$ nM min^{-1} and $K^{eff}_{M,Tx}$ values previously established for the gel beads over the range of Ficoll concentration. For translation we used Equation (1), but with mRNA as the substrate [Eq. (4)]:

$$V_{TI} = \frac{V_{max,TI}[mRNA]}{K_{M,TI} + [mRNA]} \quad (4)$$

We first modeled the translation step with a fixed $V_{max,TI}/K_{M,TI}$ value for all Ficoll concentrations (Supporting Information). This clearly did not fit our experimental data (Figure 3 A red squares and dashed black line). When fitting our experimental data by varying $K^{eff}_{M,TI}$ in a similar way as for transcription [Eq. (3)], we again found an exponential decrease in $K^{eff}_{M,TI}$, and an additional fourfold increase in translation rate. This can be explained by the increased affinity of ribosomes for mRNA (change in k_{off}/k_{on}, for instance); this is in line with the findings for transcription. The protein production rates in bulk solution, however, decreased with increasing Ficoll concentration (Fig-

ure 3B, blue circles). To explain this, we again modeled transcription and translation as a two-step Michaelis–Menten reaction, now taking into account the decreased transcription rate observed in Figure 2C. The quality of the fit suggests that the decrease in protein production can be explained by the established reduction in transcription. For translation, Ficoll therefore seems to have little or no effect.

In summary, attaching DNA to microscopic hydrogel particles with large pore sizes does not lead to changes in transcription or translation rates compared to free bulk solution. This strongly suggests that the large pore size of the hyaluronic-acid-based hydrogel allows T7 RNAP and ribosomes to diffuse freely through the hydrogel matrix. However, differences between the reactions in a hydrogel microenvironment and reactions in bulk become pronounced upon addition a macromolecular crowding agent. In a cell-like environment (inside hydrogel beads with crowding agent), the interaction probabilities of reactants increase, and volume-exclusion effects dominate. As a result k_{off}/k_{on} decreases, thus resulting in substantially lower $K^{eff}_{M,Tx}$ and $K^{eff}_{M,Tl}$ values and correspondingly higher reaction rates [Eqs. (1), (4)]. The combination of hydrogel and Ficoll can cause the reactants to undergo subdiffusion. Thus increasing Ficoll concentrations increase the rebinding events of the enzyme to its target, thereby decreasing k_{off}/k_{on}. However, if both the enzyme and the target are free to move in three dimensions, the molecules do not enter a subdiffusion regime, so the reaction will be inhibited when diffusion is decreased with increasing Ficoll concentration. Our results suggest that transcription and translation kinetics are strongly influenced by the environment, especially spatial confinement and immobility of the target at the nanometer scale. This emphasizes the importance of considering these key properties when studying reaction kinetics in different environments. Moreover, our results have strong implications for future designs of cell-free biological functions to bridge the current gap between in vitro simplicity and in vivo complexity.

Experimental Section

General experimental details: All chemicals and reagents were used as received unless otherwise noted. MilliQ water was obtained from a Water Pro PS purification system (18.1 MΩ; Labconco, Kansas City, MO). Primers for PCR and molecular beacons were obtained from Integrated DNA Technologies (Coralville, IA). Biological samples were prepared in sterile Scanlaf Mars Safety Class 2 flow boxes (Labogene, Lynge, Denmark); glassware and water were autoclaved. Thiolated hyaluronic acid was synthesized by a modified protocol[20] previously developed by Prestwich and coworkers.[29] Dialysis for removing low-molecular-weight impurities from the synthesis was performed in Spectra/Por dialysis membranes (MW cut-off: 3500 g mol^{-1}). The NMR spectrum was recorded on a Bruker AV III 600 spectrometer with D_2O as the solvent and TMS as the internal standard. The ^{1}H spectrum of thiol-functionalized hyaluronic acid is shown in Figure S1. Bright-field microscopy was performed on an IX41 microscope (Olympus) equipped with a Phantom MIRO eX2 high-speed camera (Vision Research, Wayne, NJ) in a cold room at 4 °C and low humidity. Confocal microscopy was performed on an Olympus IX81 confocal microscope equipped with an Andor iXon3 camera, Andor 400-series solid-state lasers, and a CSU-X1 spinning disk unit (Yokogawa Electric Corporation,Tokyo. Japan). eGFP and beacon molecules were excited at 488 nm, and fluorescence emission was detected through a 520/55 nm band-pass filter. Alexa 555 and the Alexa 647-labeled DNA were excited at 561 and 637 nm, respectively, and fluorescence emission was detected through 617/73 and 676/29 nm band-pass filters, respectively.

Fabrication of microfluidic devices: Stamped microfluidic devices were fabricated combining photo- and soft lithography, as shown in Figure S3.[30,31] A negative photoresist (SU-8 25 Microchem Co., Westborough, MA) was spin-coated onto a 2'' silicon wafer (Si-Mat, Kaufering, Germany). The photoresist-coated wafer was then mounted onto a mask aligner (MJB3, Süss MikroTec, Garching, Germany) and exposed to UV light (365 nm) through a transparent photomask (JD Photo-Tools, Oldham, UK) containing the desired microchannel structure. A replica in poly(dimethylsiloxane) (PDMS, height ~23 μm) was formed by mixing PDMS oligomer and crosslinker (Sylgard 184, Dow Corning) in a ratio of 10:1 (*w*/*w*) and curing the homogeneous, degassed mixture at 65 °C for 2 h. Access ports for tubing were then drilled into the replica with a biopsy needle (outer diameter: 1.0 mm, PFM, Medical, pfm medical ag, Cologne, Germany). The final microfluidic device was assembled by bonding the PDMS replica to a glass slide in a Femto oxygen plasma treatment system (60 W, 10 s; Diener electronic, Ebhausen, Germany). The bonding process was performed in an oven at 90 °C for approximately 1 h.

Fabrication of DNA-functionalized microgels by droplet microfluidics: Thiolated hyaluronic acid (1 mM) dissolved in autoclaved 1× PBS buffer (80 μL, pH 4.7) and 32xBT or eGFP DNA (40 μL) in water (350–500 ng μL^{-1}) were pre-incubated on a PCMT Thermoshaker (Grant Instruments, Shepreth, UK) at 37 °C for 75 min. Then, poly(ethylene glycol) diacrylate ($M_n \approx 575$) dissolved in degassed PBS (80 μL, 0.3%, *w*/*w*) and Alexa Fluor 555 C2 Maleimide (0.5 μL of a 1 mg mL^{-1} stock solution; Life Technologies) were added, and the pink solution was loaded into a gas-tight syringe (Hamilton 1000 series 500 μL) mounted on high-precision neMESYS syringe pumps (14.5 gear, Cetoni, Korbussen, Germany). For forming water-in-oil microdroplets, another syringe was filled with an in-house synthesized ABA copolymer surfactant (2%, *w*/*w*) dissolved in fluorinated oil (HFE-7500, 3M).[32] The syringes and a microfluidic device with flow-focusing unit (height 23 μm) with 25 μm width at the droplet-forming nozzle, were connected via PE tubing (HSE Harvard Apparatus GmbH, i.d. = 0.38 mm, o.d. = 1.09 mm). We formed hydrogel precursor microdroplets at 4 °C in a cold room by injecting water as the inner phase and fluorinated oil as the outer phase (flow rates ~200 and ~600 μL h^{-1}, respectively). The outlet tubing of the microfluidic device was fed into a Parafilm-sealed Eppendorf tube. Polymerization of the collected emulsion was achieved by heating the emulsion at 37 °C for 20 min followed by 60 °C for 40 min. The hydrogel particles were extracted from the emulsion (200 μL) by addition of 1*H*,1*H*,2*H*,2*H*-perfluorooctan-1-ol (300 μL, Sigma Aldrich 20%, *v*/*v* in HFE-7500), and water (500 μL) to transfer the particles into an aqueous phase. After phase separation and removal of the oil, the particle suspension was washed three times with aqueous L-glutamic acid potassium salt monohydrate (467 mmol), which had a comparable ionic strength to that of the home-made IVT/IVTT kits, and three times with plain water to remove any hydrogel-adhering and trapped DNA template that could later leak out of the particles.

Preparation of an IVT reaction: For gene transcription, a reaction buffer was prepared without cell lysate. It consisted of HEPES (50 mM, pH 8.0), GTP (2.4 mM), ATP (1 mM), CTP (1 mM), UTP

(1 mM), spermidine (0.66 mM), cAMP (0.5 mM), NAD (0.22 mM), coenzyme A (0.17 mM), 3-phosphoglyceric acid (3-PGA; 20 mM), folinic acid (0.045 mM), *S. cerevisiae* tRNA (0.13 mg mL^{-1}, Sigma–Aldrich), amino acids (1 mM each), magnesium glutamate (10 mM), potassium glutamate (86 mM), T7 RNA polymerase (130 U) as well as a molecular beacon (see below) for mRNA detection (0.5 μM). Ficoll 70 was subsequently added to the appropriate final concentration. The final DNA concentration encoding for the 32xBT in droplets containing beads and in bulk solution was 5 nM.

Molecular beacon sequence: /5Alex488N/mCmCmGmCmAmAmAmUmAmAmAmUmUmUmAmAmGmGmGmUmAmAmGmCmGmG/3IABkFQ/

Preparation of an IVTT reaction: The coupled transcription-translation system generally consisted of one third (*v*/*v*) cell lysate from BL21 cells (Rosetta 2) at a concentration of approximately 25 mg mL^{-1} and two thirds (*v*/*v*) of a reaction buffer stock. The final IVTT reaction mixture consisted of HEPES (50 mM, pH 8.0), GTP (2.4 mM), ATP, CTP, and UTP (1 mM each), spermidine (0.66 mM), cAMP (0.5 mM), NAD (0.22 mM), coenzyme A (0.17 mM), 3-phosphoglyceric acid (3-PGA, 20 mM), folinic acid (0.045 mM), *S. cerevisiae* tRNA (0.13 mg mL^{-1}; Sigma–Aldrich), amino acids (1 mM each), magnesium glutamate (10 mM), potassium glutamate (66 mM), T7 RNA polymerase (130 U) as well as the BL21 cell lysate (now 8.3 mg mL^{-1}, see ref. 13 for lysate preparation protocol), which contributed additional magnesium glutamate (5 mM) and potassium glutamate (20 mM), due to the buffer the lysate is prepared in. Ficoll 70 was subsequently added to the appropriate final concentration. The final DNA concentration encoding for eGFP in droplets containing beads was 10 nM.

Encapsulation of DNA-functionalized microgels into IVTT-loaded droplets: For studying gene transcription and translation in our hydrogel particles, hydrogel particles were encapsulated into IVTT-loaded microdroplets as described above, but in a 4 °C cold room. All consumables and the microfluidic device were equilibrated at 4 °C for 1 h. A homogeneous suspension of IVTT mixture (120 μL) was combined with DNA-functionalized hydrogel particles (35 μL) and stored on ice. Into a microfluidic flow-focusing device with a height and width of 50 μm at the droplet-forming nozzle, the IVTT-particle suspension was injected as the inner phase and fluorinated oil containing 2% (w/w) surfactant as the outer phase, with flow rates of the inner and outer phases at 180 and 630 μL h^{-1}, respectively. The emulsion-encapsulated hydrogel particles were directly fed into a microfluidic chamber device to minimize evaporation and allow long-term imaging. The chamber was sealed with transparent tape and transferred to the confocal microscope where the samples warmed up to room temperature and were analyzed.

Acknowledgements

We thank Frank H. T. Nelissen and Joost Groen (Radboud University, IMM) for fruitful discussions. W.T.S.H. was supported by funding from the European Research Council (ERC Adv. Grant 246812 Intercom), a VICI grant from the Netherlands Organization for Scientific Research (NWO), and by the Dutch Ministry of Education, Culture and Science (Gravity program 024.001.035).

Keywords: crowding · fluorescent probes · gene expression · hydrogel · microfluidics · spatial localization

[1] R. J. Ellis, *Trends Biochem. Sci.* **2001**, *26*, 597–604.
[2] H.-X. Zhou, G. Rivas, A. P. Minton, *Annu. Rev. Biophys.* **2008**, *37*, 375–397.
[3] G. Kolesov, Z. Wunderlich, O. N. Laikova, M. S. Gelfand, L. A. Mirny, *Proc. Natl. Acad. Sci. USA* **2007**, *104*, 13948–13953.
[4] B. R. Parry, I. V. Surovtsev, M. T. Cabeen, C. S. O'Hern, E. R. Dufresne, C. Jacobs-Wagner, *Cell* **2014**, *156*, 183–194.
[5] P. Montero Llopis, A. F. Jackson, O. Sliusarenko, I. Surovtsev, J. Heinritz, T. Emonet, C. Jacobs-Wagner, *Nature* **2010**, *466*, 77–81.
[6] O. Bénichou, R. Voituriez, *Phys. Rev. Lett.* **2008**, *100*, 168105.
[7] M. J. Morelli, R. J. Allen, P. R. ten Wolde, *Biophys. J.* **2011**, *101*, 2882–2891.
[8] E. Sokolova, E. Spruijt, M. M. K. Hansen, E. Dubuc, J. Groen, V. Chokkalingam, A. Piruska, H. A. Heus, W. T. S. Huck, *Proc. Natl. Acad. Sci. USA* **2013**, *110*, 11692–11697.
[9] F. C. Simmel, *Nat. Nanotechnol.* **2013**, *8*, 545–546.
[10] O. Bénichou, C. Chevalier, J. Klafter, B. Meyer, R. Voituriez, *Nat. Chem.* **2010**, *2*, 472–477.
[11] M. L. Mayo, E. J. Perkins, P. Ghosh, *BMC Bioinf.* **2011**, *12*, S18.
[12] S. Klumpp, M. Scott, S. Pedersen, T. Hwa, *Proc. Natl. Acad. Sci. USA* **2013**, *110*, 16754–16759.
[13] M. M. K. Hansen, L. H. H. Meijer, E. Spruijt, R. J. M. Maas, M. V. Rosquelles, J. Groen, H. A. Heus, W. T. S. Huck, *Nat Nanotechnol.* **2015**, doi:10.1038/nnano.2015.243.
[14] J. Elf, G.-W. Li, X. S. Xie, *Science* **2007**, *316*, 1191–1194.
[15] I. Izeddin, V. Récamier, L. Bosanac, I. I. Cissé, L. Boudarene, C. Dugast-Darzacq, F. Proux, O. Bénichou, R. Voituriez, O. Bensaude, M. Dahan, X. Darzacq, *eLife* **2014**, *3*, e02230.
[16] X. Ge, D. Luo, J. Xu, *PLoS One* **2011**, *6*, e28707.
[17] B. Meyer, O. Bénichou, Y. Kafri, R. Voituriez, *Biophys. J.* **2012**, *102*, 2186–2191.
[18] I. Golding, E. C. Cox, *Phys. Rev. Lett.* **2006**, *96*, 098102.
[19] D. S. Banks, C. Fradin, *Biophys J.* **2005**, *89*, 2960–2971.
[20] J. Thiele, Y. Ma, D. Foschepoth, M. M. K. Hansen, C. Steffen, H. A. Heus, W. T. S. Huck, *Lab Chip* **2014**, *14*, 2651–2656.
[21] R. Gabler, E. W. Westhead, N. C. Ford, *Biophys. J.* **1974**, *14*, 528–545.
[22] J. Shin, V. Noireaux, *J. Biol. Eng.* **2010**, *4*, 8.
[23] F. Courtois, L. F. Olguin, G. Whyte, D. Bratton, W. T. S. Huck, C. Abell, F. Hollfelder, *ChemBioChem* **2008**, *9*, 439–446.
[24] D. Y. Vargas, A. Raj, S. A. E. Marras, F. R. Kramer, S. Tyagi, *Proc. Natl. Acad. Sci. USA* **2005**, *102*, 17008–17013.
[25] S. B. Zimmerman, A. P. Minton, *Annu. Rev. Biophys. Biomol. Struct.* **1993**, *22*, 27–65.
[26] H. Kim, M. Yang, M.-U. Choi, K. J. Shin, *J. Chem. Phys.* **2001**, *115*, 1455–1459.
[27] J. A. Dix, A. S. Verkman, *Annu. Rev. Biophys.* **2008**, *37*, 247–263.
[28] E. Spruijt, E. Sokolova, W. T. S. Huck, *Nat. Nanotechnol.* **2014**, *9*, 406–407.
[29] X. Z. Shu, Y. Liu, Y. Luo, M. C. Roberts, G. D. Prestwich, *Biomacromolecules* **2002**, *3*, 1304–1311.
[30] J. C. McDonald, G. M. Whitesides, *Acc. Chem. Res.* **2002**, *35*, 491–499.
[31] R. Martinez-Duarte, M. J. Madou, *Microfluidics and Nanofluidics Handbook, Vol. 2* (Ed.: S. K. Mitra, S. Chakraborty), CRC Press, Boca Raton, **2011**.
[32] V. Chokkalingam, J. Tel, F. Wimmers, X. Liu, S. Semenov, J. Thiele, C. G. Figdor, W. T. S. Huck, *Lab Chip* **2013**, *13*, 4740–4744.

Manuscript received: October 21, 2015
Accepted article published: November 25, 2015
Final article published: December 17, 2015